



HAL
open science

Two-stroke scooters are a dominant source of air pollution in many cities

S. M. Platt, I. El Haddad, S. M. Pieber, R. -J. Huang, A. A. Zardini, M. Clairotte, R. Suarez-Bertoa, P. Barmet, L. Pfaffenberger, R. Wolf, et al.

► **To cite this version:**

S. M. Platt, I. El Haddad, S. M. Pieber, R. -J. Huang, A. A. Zardini, et al.. Two-stroke scooters are a dominant source of air pollution in many cities. *Nature Communications*, 2014, 5, 10.1038/ncomms4749 . hal-01456406

HAL Id: hal-01456406

<https://hal.science/hal-01456406>

Submitted on 17 Jan 2018

HAL is a multi-disciplinary open access archive for the deposit and dissemination of scientific research documents, whether they are published or not. The documents may come from teaching and research institutions in France or abroad, or from public or private research centers.

L'archive ouverte pluridisciplinaire **HAL**, est destinée au dépôt et à la diffusion de documents scientifiques de niveau recherche, publiés ou non, émanant des établissements d'enseignement et de recherche français ou étrangers, des laboratoires publics ou privés.

ARTICLE

Received 12 Oct 2013 | Accepted 28 Mar 2014 | Published 13 May 2014

DOI: 10.1038/ncomms4749

Two-stroke scooters are a dominant source of air pollution in many cities

S.M. Platt¹, I. El Haddad¹, S.M. Pieber¹, R.-J. Huang¹, A.A. Zardini², M. Clairotte^{2,†}, R. Suarez-Bertoa², P. Barmet¹, L. Pfaffenberger¹, R. Wolf¹, J.G. Slowik¹, S.J. Fuller³, M. Kalberer³, R. Chirico^{1,†}, J. Dommen¹, C. Astorga², R. Zimmermann^{4,5}, N. Marchand⁶, S. Hellebust⁶, B. Temime-Roussel⁶, U. Baltensperger¹ & A.S.H. Prévôt¹

Fossil fuel-powered vehicles emit significant particulate matter, for example, black carbon and primary organic aerosol, and produce secondary organic aerosol. Here we quantify secondary organic aerosol production from two-stroke scooters. Cars and trucks, particularly diesel vehicles, are thought to be the main vehicular pollution sources. This needs re-thinking, as we show that elevated particulate matter levels can be a consequence of 'asymmetric pollution' from two-stroke scooters, vehicles that constitute a small fraction of the fleet, but can dominate urban vehicular pollution through organic aerosol and aromatic emission factors up to thousands of times higher than from other vehicle classes. Further, we demonstrate that oxidation processes producing secondary organic aerosol from vehicle exhaust also form potentially toxic 'reactive oxygen species'.

¹Laboratory of Atmospheric Chemistry, Paul Scherrer Institute, CH-5232 Villigen, Switzerland. ²European Commission Joint Research Centre, Institute for Energy and Transport, 21027 Ispra, Italy. ³Centre for Atmospheric Science, Department of Chemistry, University of Cambridge, Cambridge CB2 1EW, UK. ⁴Cooperation Group comprehensive molecular analytics/Joint Mass Spectrometry Centre, Helmholtz Zentrum München, 85764 Neuherberg, Germany. ⁵Chair of Analytical Chemistry/Joint Mass Spectrometry Centre, Institute of Chemistry, University of Rostock, 18051 Rostock, Germany. ⁶Aix Marseille Université, CNRS, LCE FRE 3416, 13331 Marseille, France. † Present addresses: INRA, UMR Eco and Sols, 2 Place Pierre Viala, 34060 Montpellier, France (M.C.); Italian National Agency for New Technologies, Energy and Sustainable Economic Development (ENEA), UTAPRAD-DIM, Via E. Fermi 45, 00044 Frascati, Italy (R.C.). Correspondence and requests for materials should be addressed to A.S.H.P. (email: andre.prevot@psi.ch).

Particulate matter (PM) damages health¹ and affects climate². Road vehicles are a significant source of PM, particularly in urban areas. A number of recent studies have shown that a large fraction, possibly the largest, of vehicular PM is secondary organic aerosol (SOA) produced via atmospheric oxidation of precursor gases in the exhaust^{3–5}. Thus, understanding vehicular air pollution requires an assessment of SOA formation from different vehicle types. Two-stroke (2S) scooters (powered two-wheeled vehicles with engine displacement $\leq 50\text{ cm}^3$) are popular globally, particularly in Asia, Africa and Southern Europe. Despite being high emitters of primary PM^{6,7}, regulations for scooters are generally less stringent than for other vehicles, for example, in Europe having reached Euro 5/V (a fifth tranche of regulations), for passenger cars and trucks, versus only Euro 2 for scooters (see Supplementary Table 1 and ref. 8). Accordingly, a scientific report to the European Commission suggests that scooters will emit more volatile organic compounds (VOCs) than all other vehicles combined in Europe by 2020 (ref. 9). Furthermore, high PM levels and toxic aromatic hydrocarbons, important SOA precursors¹⁰, have been observed in many cities, especially in Asia¹¹. Globally, organic aerosol (OA) dominates PM, with SOA accounting for the largest fraction⁴.

Here we show that 2S scooters emit significant amounts of primary organic aerosol (POA), aromatic VOCs and also produce significant SOA. We use the term ‘asymmetric polluter’ to describe these vehicles as their emission factors (EFs) and evidence from air quality measurements before and after bans on

scooters in Asian cities suggest they may dominate vehicular pollution despite their relatively small numbers. Chemical analysis of the emissions shows that SOA is mainly produced via photo-oxidation of aromatic VOCs, present in gasoline, from the exhaust. This shows that the known issue of incomplete fuel combustion during the 2S cycle is also responsible for SOA formation. Finally, we present the first online measurements of aged exhaust showing that SOA formation also produces reactive oxygen species (ROS) with potentially detrimental effects on our lungs.

Results

Emission Factors. We investigated POA emissions and SOA formation from 2S scooters and their potential health effects. The oxidation of VOCs in 2S scooter emissions produces significant SOA (g carbon (C) kg^{-1} fuel), with total OA on average 2.9 and 2.4 times higher than POA after aging for idling and driving 2S scooters, respectively (Fig. 1, and Supplementary Table 2). In addition, substantial toxic aromatic emissions (up to $\sim 40\%$ of emitted VOC volume for the scooters of this study) of benzene, toluene and C2–C4 alkylated benzenes, which are recognized SOA precursors^{10,12}, are present in the exhaust. Among the aromatics, benzene is of particular concern due to its carcinogenicity. Levels in the raw 2S scooter exhaust were as high as $300,000\ \mu\text{g m}^{-3}$ or 146 p.p.m.(v) from idling. The EU annual mean limit for the protection of human health is $5\ \mu\text{g m}^{-3}$ (ref. 13), while the US National Institute for

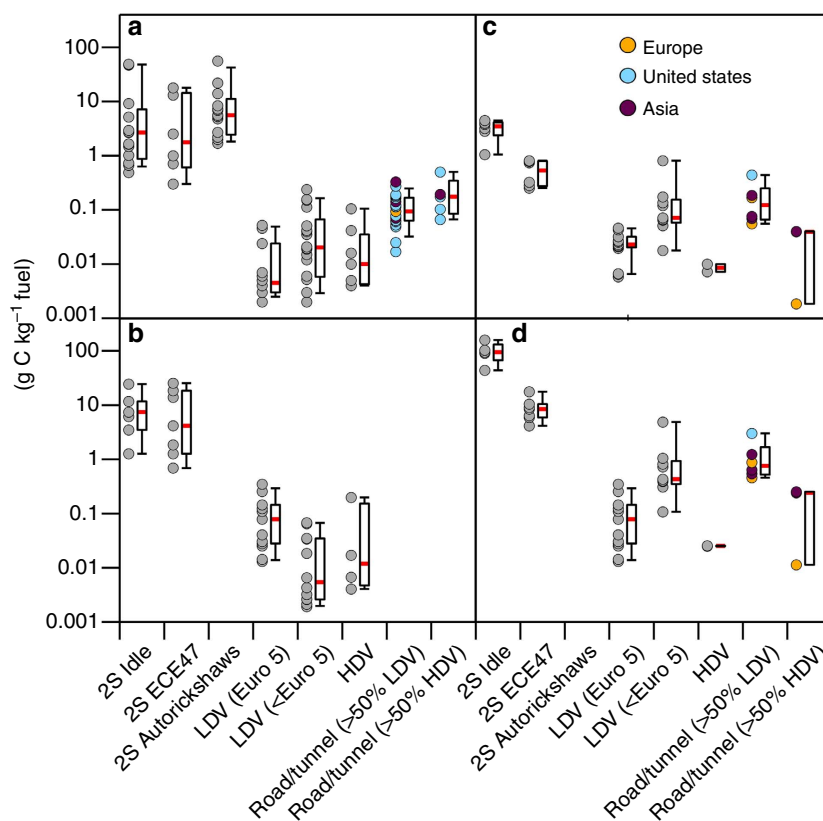


Figure 1 | Emission factors from scooters and other vehicles. EFs plotted as box-and-whiskers (median line, red; 25th and 75th percentile, box; 10th and 90th percentile, whiskers) of (a) POA, (b) aged OA (POA + SOA formation), (c) benzene and (d) light aromatics (benzene, toluene and C2–C4 alkylated benzenes). Points shown next to the box-and-whiskers are the individual data points, coloured depending on measurement region for ambient data. 2S scooters (this study, $n = 3$) were run in idle or during driving cycles (ECE47). Data on the other vehicles shown are from the literature (Supplementary Table 3) for light-duty and heavy-duty vehicles (LDVs and HDVs). LDVs data are further divided between vehicles meeting Euro 5 and those not meeting Euro 5, labelled <Euro 5 in parenthesis. Ambient data are split according to a contribution of HDVs to the data of higher than or lower than 50%. Note that many of the higher ambient values are from older vehicle studies (Supplementary Table 3).

Occupational Safety and Health recommends that workers wear special breathing equipment when exposed to benzene at levels exceeding 1 p.p.m. for 15 min. Waiting in traffic behind a 2S scooter, for example, at junctions and while the scooter is idling, may therefore be highly deleterious to health.

Secondary organic aerosol yields. The contribution of the aromatics to SOA formation was estimated by calculating an apparent aerosol yield, y_{apparent} , assuming all SOA comes from aromatic precursors:

$$y_{\text{apparent}} = C_{\text{SOA}} / \sum_i \Delta_i \quad (1)$$

where C_{SOA} is the SOA produced ($\mu\text{g m}^{-3}$) for a given mass change in aromatic i (Δ_i , i = benzene, toluene or C2–C4 alkylated benzenes). Apparent yields closely match average concentration-weighted literature aromatic SOA yields¹⁰ (Fig. 2a, Supplementary Note 1) for idling, complete ECE47 driving cycles and ECE47 phase one (Ph1), indicating that most SOA is from aromatic precursors (Fig. 2a). SOA from ECE47 phase two (Ph2) alone is underestimated by equation (1), suggesting SOA production from unidentified compounds, emitted by the hot engine. Note that the total emission during a full cycle is dominated by Ph1, that is, by cold engine emissions. Furthermore, a ‘Van Krevelen diagram’ illustrates the aging of 2S scooter emissions, from oxygen to carbon (O:C) ~ 0 to O:C ~ 0.6 . This elemental composition is consistent with that of previously observed SOA from aromatic precursors¹⁴ (Fig. 2b). We therefore conclude that SOA formation from 2S scooter emissions is likely from the oxidation of aromatics, in contrast to diesel SOA, which is predominantly from other precursors¹⁵.

Comparison to other vehicle types and ambient data. Figure 1 also shows laboratory and ambient measurements of POA, light aromatic and benzene EFs from passenger cars and trucks (Supplementary Table 3). Ambient data are from roadside/tunnel measurements in the US, EU and Asia, and are split according to the fraction of light-duty and heavy-duty vehicles (LDVs and HDVs, respectively) at the measurement site. Note that the general trend is for lower EFs in newer studies, consistent with improvements in emission controls. Also shown are data from Indian in-use 2S autorickshaws for comparison to the European scooters of this study. Caution is required in such a comparison; however, although similar (both have 2S engines), these are a different vehicle class and were furthermore tested during a different driving cycle. In general, ambient EFs from Asian vehicles are in the same range as European and US vehicles, while emissions from in-use 2S rickshaws are slightly higher than from the European scooters of this study. POA emissions from 2S scooters are on average around 20 (maximum 2,780) times higher than ambient (light-duty dominant) values, and aged OA emissions on an average 53–771 times higher than laboratory studies on other vehicle types. It should be noted that absolute aerosol concentrations can influence EFs: higher measurement concentrations would lead to higher EFs¹⁵. SOA formation is most significant from idling scooter emissions, while smaller at higher engine loads. However, POA emissions are higher under the latter conditions, and the aggregate POA + SOA emission at high load is comparable with that from idling.

Reactive oxygen species. We also examined the health implications of the 2S scooter SOA (other than those from the mass increase) using online measurements of particle-bound, water soluble reactive oxygen species (ROS)¹⁶, which are linked to negative health effects¹⁷. ROS are undetectable in POA, but

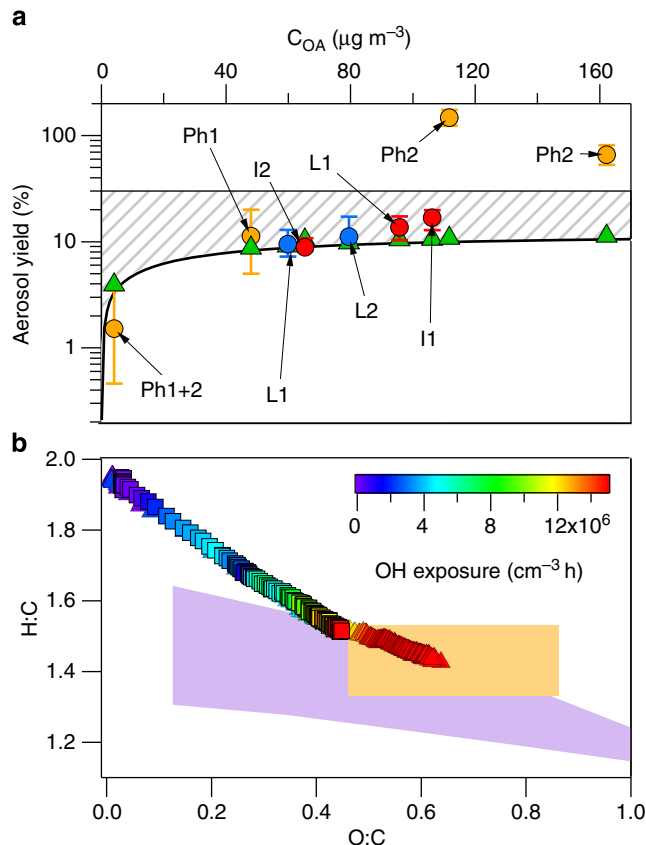


Figure 2 | Contribution of aromatic oxidation to two-stroke scooter secondary aerosol formation. (a) Apparent SOA mass yields, y_{apparent} (equation (1)), as a function of suspended OA concentration (C_{OA}). Error bars show the sensitivity of y_{apparent} to the chamber wall-loss factor, \pm one s.d. y_{apparent} for a Euro 1 and two Euro 2 2S scooters are shown in red, blue and orange, respectively. Ph 1 and Ph 2 are the first and second phases of the ECE47 driving cycle, I and L refer to idling and simulated low power, respectively. A predicted yield, concentration-weighted, for the mixture of all aromatics (Supplementary Note 1), is given in green triangles. The shaded region denotes the range between maximum (low NO_x) and minimum (high NO_x) SOA yields for *m*-xylene, a major aromatic constituent of gasoline. (b) Elemental ratios of OA emissions for the Euro 1 (squares) and a Euro 2 (triangles) scooter as a function of photochemical age. Elemental ratios observed for xylene¹³ and ambient³¹ SOA are shown, orange and purple, respectively.

accounts for 0.5–1% carbon in the aged OA, suggesting that PM emissions initially become increasingly toxic with aging (Fig. 3). Increasing ROS is consistent with the increased O:C ratio of the aerosol and in line with a previous study showing increased oxidative potential with aging for 2S scooter emissions, albeit at aerosol and oxidant loadings much higher than under ambient conditions¹⁸. After 1–2 h of irradiation, ROS stabilizes or decreases, as reported previously for organic peroxides, likely due to decomposition processes^{19,20}.

Discussion

There are likely several reasons for these relatively large OA and aromatic emissions from 2S scooters. First, 2S engines, unlike four-stroke (4S), require addition of lubricant oils to the fuel, some of which is emitted in the exhaust. Second, during the 2S engine cycle some of the fresh fuel/air mixture passes directly through the engine²¹, increasing VOC emissions, which may

explain the high SOA formation. Third, scooters generally utilize 'rich combustion' (low-air/fuel ratio), improving drivability while producing higher CO, VOC and PM emissions (but lower NO_x). Accordingly, the VOC emissions measured here, in particular aromatics as found in raw gasoline, are also on average 124 and 11 times higher from idling and driving 2S scooters, respectively,

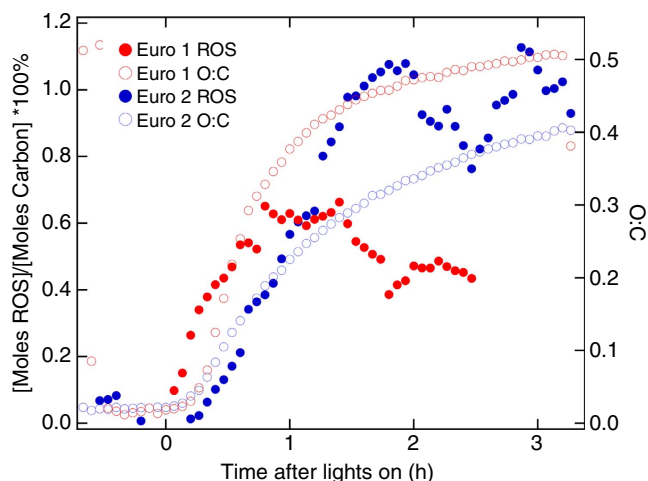


Figure 3 | Reactive oxygen species in two-stroke scooter emissions. The percentage of water soluble reactive oxygen species (ROS) and elemental O:C ratios of organic aerosol as a function of time after lights on in the smog chamber from Euro 1 (red) and Euro 2 (blue) 2S scooter exhaust emissions. ROS concentration measured in moles hydrogen peroxide equivalents is normalized to the molar organic carbon concentration per m^3 inside the smog chamber to give a percentage.

compared with those from other vehicles. Finally, scooter after-treatment systems are inherently inefficient due to their relatively small size and longer light-off times.

Precise estimation of a relative contribution to vehicular PM and aromatics from 2S scooters is difficult, since vehicle regulations vary by country. Another complication arises from the possibility of large contributions to OA from a small number of super-polluting vehicles (of all types). However, many scooters will likely fall into this super-polluting category, especially as a considerable number of scooters are in operation in some regions without any form of emissions control (note that all scooters presented in this study are equipped with two-way oxidation catalysts, which reduce emissions of carbon monoxide and VOCs) and because emissions may be further exacerbated by poor maintenance and tampering, rife for scooters²². Furthermore, ambient data in Fig. 1 likely include a number of such super-polluting vehicles. Therefore, our results suggest that 2S scooters are 'asymmetric polluters' of OA and aromatics compared with other vehicles. Using the average 2S scooter EF (ECE47 driving cycle) in Fig. 1 suggests that 2S scooters contribute to around 60% of roadside POA in Bangkok, where they account for 10% of fuel consumption (Fig. 4). In a more extreme case (comparing the 75th percentile for scooters and 25th percentile for ambient light-duty dominated), 2S scooters would contribute over 96% to roadside POA. Note that these values are based on the European scooters of this study. As Fig. 1 shows, emissions from some in-use Asian 2S vehicles may be higher, by a factor of three. Since other Asian vehicles are not expected to be more polluting based on Fig. 1, higher emissions from in-use Asian 2S vehicles would strengthen our conclusion that 2S scooters dominate urban pollution in the region.

Estimation of contributions to aged OA is more difficult as vehicular SOA has not been systematically quantified under

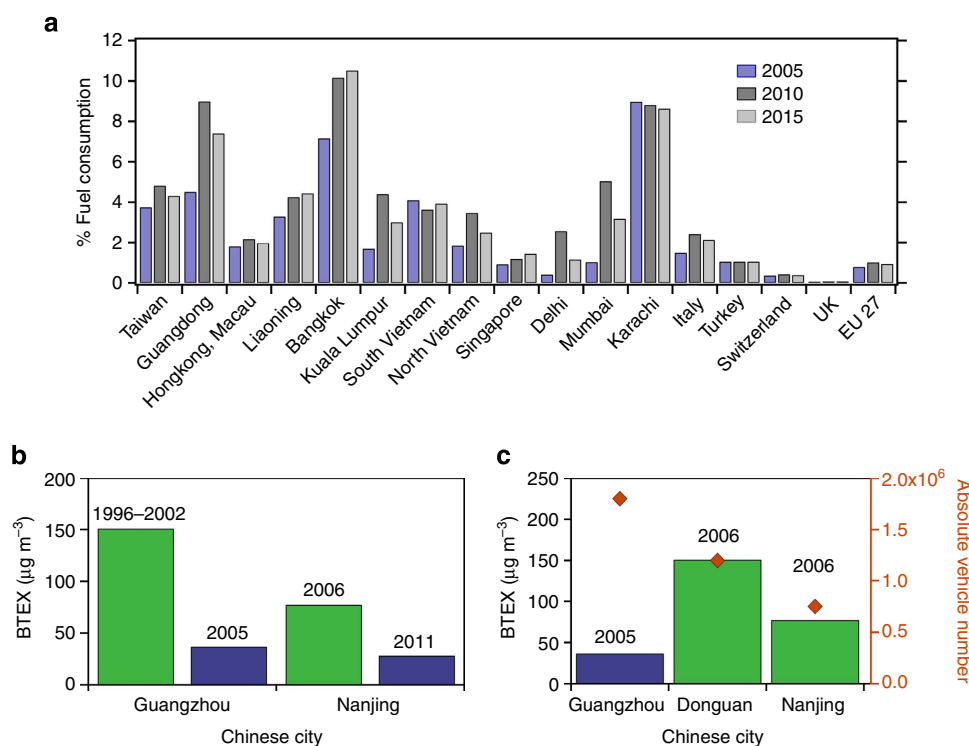


Figure 4 | Ambient and model data on two-stroke scooters. (a) Share of total fuel consumption by 2S scooters in 2005, 2010 and 2015 from the Greenhouse gas Air pollution Interactions and Synergies, GAINS, model³¹. (b) Roadside benzene, toluene, ethyl-benzene and xylene (BTEX) before (green) and after (blue) banning/restricting 2S scooters in two Chinese cities (c) Roadside BTEX and number of all vehicles in three Chinese cities, before (green) and after (blue) banning/restricting 2S scooters.

ambient conditions. However, smog chamber measurements suggest average-aged OA contributions to ambient vehicular PM of 85% (comparing with LDVs meeting Euro 5) or 98% (comparing with LDVs meeting less than Euro 5) from 2S scooters. Meanwhile, in the EU, 2S scooters consume only 1% of vehicle fuel, Fig. 4. Even with these low numbers, scooters may be the major source of some of the vehicle-related pollutants, especially in Southern Europe, and our data suggest that reducing the numbers of these vehicles would cost-effectively mitigate vehicle OA and aromatic emissions, given the alternatives available (electric and 4S). In this regard China has taken the lead, banning or restricting scooters in many cities since the late 1990s²³, leading to large decreases in the traffic-related aromatic emissions in some Chinese cities (Fig. 4b). Strikingly, roadside aromatics are now higher in Dongguan, where scooters are not banned, than 60 km away in Guangzhou, even though the traffic volume is much higher in Guangzhou (Fig. 4c). This result is statistically significant: year-to-year benzene, toluene, ethylbenzene and xylene concentrations in Guangzhou were $229 \mu\text{g m}^{-3}$ in 1996, $244 \mu\text{g m}^{-3}$ in 1999, $290 \mu\text{g m}^{-3}$ in 2000 and $150 \mu\text{g m}^{-3}$ in 2002, average 228 ± 68 versus $37 \mu\text{g m}^{-3}$ after the scooter ban in 2005, for example. Benzene, toluene, ethylbenzene and xylene concentrations for Guangzhou and other cities reported in the literature are given in Supplementary Table 4.

Our data suggest that 2S scooters are a significant, and in many cities the largest, source of vehicular PM and toxic SOA and aromatic hydrocarbons, despite being a relatively small fraction of the total fleet. Therefore, given the alternative technologies available, restrictions on 2S scooters, already implemented in China, could improve air quality in many cities around the globe.

Methods

Measurement campaigns. We combine results from two measurement campaigns where 2S scooter exhaust was injected through a heated inlet into smog chambers^{3,24,25} to produce SOA via photochemistry. During the first study, an

in-use Euro 1 (E1) and a new Euro 2 (E2a) 2S scooter were run in idle or simulated low power. During the second campaign, emissions from a different Euro 2 2S scooter (E2b) were sampled during ECE47 driving cycles²⁶. Supplementary Table 5 provides specifications of these vehicles. European (exhaust) emission standards are shown in Supplementary Table 1. Average OH concentrations were $\sim 5 \times 10^6 \text{ cm}^{-3}$. OH concentrations were determined from the decay of a nine times deuterated butanol (butanol-D9, 98% Aldrich) tracer as measured using a quadrupole proton transfer reaction mass spectrometer (idling 2S scooters) or proton transfer reaction time-of-flight mass spectrometer (Ionicon Analytik, driving cycle 2S scooters), see also ref. 27.

Estimation of the NO_x regime during experiments. Experiments were under 'high NO_x' conditions, which we define as the chemical regime where the main reactions of peroxy radicals (RO₂) are with NO rather than other peroxy radicals (self-reaction, or reaction with hydroperoxy radicals). An estimate of the ratio of the RO-forming reactions (RO₂ + NO) versus peroxide-forming reactions (RO₂ + RO₂, RO₂ + HO₂) is possible for experiments conducted on idling scooters at the Paul Scherrer Institute chamber, instrumentation for which includes a NO_x monitor equipped with a 'blue light converter' (ensuring NO_x is truly measured as NO₂ + NO). Figure 5b shows the measured concentrations of NO and O₃, from an experiment conducted on 22 November 2010. This experiment was typical, with an initial VOC:NO_x ratio of around 50 and continuous addition of NO during photochemical aging.

The concentration of NO as a function of time t is given by:

$$\frac{d[\text{NO}]}{dt} = j_{\text{NO}_2}[\text{NO}_2] - k_1[\text{NO}][\text{O}_3] - k_2[\text{NO}][\text{RO}_2 + \text{HO}_2], \quad (2)$$

Where j_{NO_2} is the photolysis rate of NO₂ in the smog chamber (0.01 s^{-1}) and k_1 ($1.8 \times 10^{-14} \text{ cm}^3 \text{ molecule}^{-1} \text{ s}^{-1}$) and k_2 ($7.7 \times 10^{-14} \text{ cm}^3 \text{ molecule}^{-1} \text{ s}^{-1}$) are the reaction rate constants for NO with O₃ and peroxides (CH₃O₂) at 298 K, respectively. Assuming a steady state of NO (only an approximation, Fig. 5 indicates this point is not reached until around 15 h of OH exposure (at OH = 10^6 molecules cm⁻³)), equation (2) can be written:

$$[\text{RO}_2 + \text{HO}_2] = \frac{j_{\text{NO}_2}[\text{NO}_2] - k_1[\text{NO}][\text{O}_3]}{k_2[\text{NO}]} \quad (3)$$

Equation (3) suggests NO concentrations at least an order of magnitude higher than RO₂ + HO₂ (for example, 14 times higher at OH = 10×10^6 molecules cm⁻³ h) during the experiment, based on concentrations measured inside the chamber (Fig. 5).

The branching ratio r between the RO₂/HO₂ reactions with NO versus other with peroxides (Fig. 5a) is determined using

$$r = \frac{k_2[\text{NO}]}{k_3[\text{HO}_2 + \text{RO}_2]}, \quad (4)$$

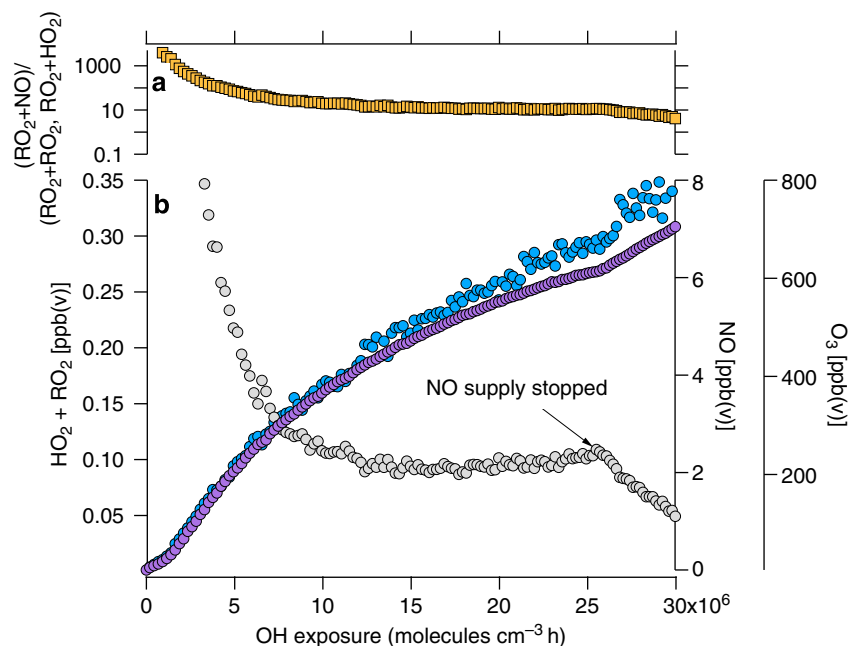


Figure 5 | Estimation of NO_x regime. (a) Calculated branching ratio between nitrate and peroxide reactions (orange squares) in the smog chamber during aging of emissions from an idling 2S scooter and (b) measured concentrations of ozone (O₃) (purple circles) and nitrogen monoxide (NO) (grey circles) as well as calculated peroxy radical (HO₂ + RO₂) (blue circles) concentrations.

where k_3 is the reaction rate constant between HO_2 and CH_3O_2 ($7.7 \times 10^{-12} \text{ cm}^3 \text{ molecule}^{-1} \text{ s}^{-1}$) at 298 K. We assume that the concentration of HO_2 and RO_2 is the same.

Figure 5a illustrates that the NO pathway is dominant, by at least a factor of 20 until $\text{OH} = 10 \times 10^6 \text{ molecules cm}^{-3} \text{ h}$, and by initially thousands of times higher, over the peroxide pathway. Since $r \gg 1$ we consider these experiments 'high NO_x '.

An estimation of r during the tests on driving cycle emissions is complicated by the lack of an accurate NO_x instrument (that is, one equipped with a blue light converter). Furthermore, NO was only continuously added during the experiment where emissions were sampled from the cold phase (which featured the highest VOC: NO_x ratio of any experiment). However, given that the driving cycle tests generally produced higher NO emissions than the idling tests, and given that most fall on the yield curve in Fig. 2, we also assume $r \gg 1$, although we can not rule out that during some experiments the conditions change from high to low NO_x . Although the VOC: NO_x ratios were high (around 50), our best estimate suggests that idling experiments were high NO_x throughout. Figure 5b shows the measured concentrations of NO and O_3 , during the experiment.

Idling scooter experiments. Emissions were introduced into the 27 m³ Paul Scherrer Institute Teflon environmental chamber²⁴. The external temperature of the scooter exhaust was monitored (Thermocouple type K, Messelemente) and after an initial warming period of several minutes (consisting of idling or applying low power) the emissions were injected only when the external exhaust temperature was stable at idle or at simulated low power. Supplementary Table 2 provides the operating conditions, smog chamber OA concentrations and aerosol EFs of this study used in Fig. 1.

OA was monitored with a high-resolution time-of-flight aerosol mass spectrometer (Aerodyne). Unity collection efficiency is assumed, since emitted particles likely consist of spherical oil-like droplets with low bounce. After an initial spike in the OA concentration following sample injection, a time of at least 20 min was allowed for equilibration. The concentration of OA after this point was taken as the initial POA emission. A battery of $80 \times 100 \text{ W}$ ultraviolet black lights (ErgoLine 'Cleo Performance', Solarium lights), was used to initiate photo-oxidation and SOA formation. Experiments were carried out with a steady injection of NO ($< 20 \text{ ml min}^{-1}$) whereby NO was maintained at around 2–3 ppb(v). Relative humidity inside the smog chamber was between 40–60% for all experiments, and temperature was maintained at 25 °C.

OA was corrected for wall losses using

$$\text{OA}_{\text{WLC}}(t) = \frac{\text{OA}_{\text{MEAS}}(t)}{\exp(-kt)}, \quad (5)$$

where $\text{OA}_{\text{WLC}}(t)$ and $\text{OA}_{\text{MEAS}}(t)$ are the wall-loss corrected and measured organic matter concentrations, respectively, as a function of time t , and k is the first order mass-loss rate constant determined from an exponential fit of BC data.

VOCs inside the smog chamber were quantified with a quadrupole proton transfer reaction mass spectrometer, while carbon monoxide was quantified with a dedicated CO monitor (Aerolaser, CO-Monitor AL5002) and total gas-phase hydrocarbons were measured from the chamber using a flame ionization detector (FID, J.U.M model VE 7). Additional measurements at the tailpipe were performed by transferring emissions through a heated line (191 °C) to a Fourier transformed infrared spectrometer (MKS Multigas analyser 2030) for online measurements (at 1 Hz) of small hydrocarbons, nitrogen containing species (NO, NO_2 , N_2O , NH_3 and HCN) and other oxygenated small organics (formaldehyde, acetaldehyde), as well as CO and CO_2 .

Online reactive oxygen species measurements. Online particle-bound ROS analysis utilized the fluorescence probe 2,7-dichlorofluorescein in solution. Particles were collected and continuously extracted on a wetted hydrophilic filter. The particle collector samples air at 51 min^{-1} and collects particles larger than aerodynamic diameter 50 nm with greater than 95% efficiency. Particles are collected and extracted in an aqueous solution of horseradish peroxidase (0.5 U ml^{-1}) allowing immediate reaction of ROS on collection. The concentration of ROS is characterized following subsequent reaction of the oxidized horseradish peroxidase with 2,7-dichlorofluorescein ($5 \mu\text{M}$) for 10 min at 40 °C, yielding the fluorescent product DCF in the continuous flow set up. The concentration of 2,7-dichlorofluorescein is measured using fluorescence spectroscopy in a flow-through cell and calibrated to ROS concentration with hydrogen peroxide. ROS data in Fig. 3 are normalized to the total carbon m^{-3} , determined from high-resolution fitting of aerosol mass spectrometer data, and presented as a percentage.

Driving cycle scooter experiments. The Paul Scherrer Institute mobile smog chamber³ was deployed, and experiments conducted in a certified chassis dynamometer test cell (Vehicle Emissions Laboratories, Joint Research Centre of the European Commission, JRC-Ispra, Italy)^{28,29}. Emissions from 2S scooters were sampled at the tailpipe during full ECE47 driving cycles, during Ph1 only of the ECE47 (first four modules of the driving cycle, Ph1), and during Ph2 only of the ECE47 (final four modules of the driving cycle, Ph2). The emissions were transferred to the smog chamber via a heated inlet system (150 °C) and Dekati ejector dilutor. Ultraviolet lights were switched on after several minutes to initiate

photochemistry. OA concentrations were measured with a high-resolution time-of-flight aerosol mass spectrometer (Aerodyne), while black carbon was quantified with an aethalometer (AE33, Aerosol d.o.o.). The exponential decay rate of black carbon k was used in equation (5) to correct for particle losses to the walls. Gas-phase compounds were monitored with a proton transfer reaction time-of-flight mass spectrometer (Ionicon), while CO_2 and CO were measured using a cavity ring down spectrometer (Picarro, G2401) and total hydrocarbons were measured with a flame ionization detector (Horiba, THC Monitor APHA-370).

Emission factor determination. EFs from both measurement campaigns (EF, $\text{g C kg}^{-1} \text{ fuel}$), (see also Supplementary Table 3), were calculated using a carbon mass balance:

$$\text{EF} = \left(\frac{\text{OC}}{\text{C}_{\text{CO}_2} + \text{C}_{\text{CO}} + \text{C}_{\text{HC}}} \right) \cdot W_c, \quad (6)$$

where C denotes carbon mass, and the subscripts CO_2 , CO, HC, carbon dioxide, carbon monoxide and hydrocarbon, respectively. W_c is the fuel carbon content (0.847 for gasoline).

For the idling scooter experiments, C_{CO} and C_{CO_2} were measured at the tailpipe using the Fourier transformed infrared spectrometer. C_{HC} was measured from the smog chamber and scaled-up to the tailpipe concentration using the dilution ratio $\text{CO}_{\text{tailpipe}}/\text{CO}_{\text{smog chamber}}$. Meanwhile, for the driving cycles all concentrations were determined at the smog chamber.

Emission factors from the literature. Figure 1 and Supplementary Table 3 show EFs calculated from the literature. When available, EFs are given as reported. OA EFs measured in tunnels/roadside are assumed to consist purely of POA and are converted to EFs in units of $\text{g kg}^{-1} \text{ fuel}$ using an organic matter to organic carbon ratio (OM:OC) of 1.2 (ref. 30). EFs given in units of g km^{-1} are converted using the following fuel consumptions (km kg^{-1}): Asia LDVs: 16.43; US LDVs: 14.93; EU LDVs: 18.20; Heavy-duty vehicles: 2.85. EFs measured during the Kansas City vehicle study are estimated by inserting per km EFs into equation (6). SOA in Supplementary Table 3 ($\text{g C kg}^{-1} \text{ fuel}$) is converted from units of $\text{g kg}^{-1} \text{ fuel}$ using an OM:OC ratio of 2.0 (ref. 30). SOA formation from 2S scooters is not available in the literature, but was estimated from emissions of aromatic hydrocarbons using a yield (see Supplementary Note 1 and Fig. 2) of 8.4% (suspended OA concentration $50 \mu\text{g m}^{-3}$). Further notes to individual studies are also provided in Supplementary Table 3.

References

- Dockery, D. W. *et al.* An association between air pollution and mortality in six US cities. *New Engl. J. Med.* **329**, 1753–1759 (1993).
- IPCC. *Contribution of Working Group I to the Fourth Assessment Report of the Intergovernmental Panel on Climate Change* (Cambridge University Press, 2007).
- Platt, S. M. *et al.* Secondary organic aerosol formation from gasoline vehicle emissions in a new mobile environmental reaction chamber. *Atmos. Chem. Phys.* **13**, 9141–9158 (2013).
- Hallquist, M. *et al.* The formation, properties and impact of secondary organic aerosol: current and emerging issues. *Atmos. Chem. Phys.* **9**, 5155–5236 (2009).
- Nordin, E. Z. *et al.* Secondary organic aerosol formation from idling gasoline passenger vehicle emissions investigated in a smog chamber. *Atmos. Chem. Phys.* **13**, 6101–6116 (2013).
- Czerwinski, J., Comte, P. & Reutimann, F. Nanoparticle Emissions of a DI 2-Stroke Scooter with Varying Oil and Fuel Quality. *SAE transactions* **114**, 541–556 (2005).
- Rijkeboer, R., Bremmers, D., Samaras, Z. & Ntziachristos, L. Particulate matter regulation for two-stroke two wheelers: necessity or haphazard legislation? *Atmos. Environ.* **39**, 2483–2490 (2005).
- European Commission (EC). *O.J.E.C.* **L67**, 14–30 (2002).
- Geivanidis, S. *et al.* Aristotle University (2008). *Thessaloniki*, available at http://www.ec.europa.eu/enterprise/sectors/automotive/documents/calls-for-tender-and-studies/index_en.htm, last accessed 12 January 2014.
- Ng, N. L. *et al.* Secondary organic aerosol formation from m-xylene, toluene, and benzene. *Atmos. Chem. Phys.* **7**, 3909–3922 (2007).
- Lan, T. T. N. & Minh, P. A. BTEX pollution caused by motorcycles in the megacity of HoChiMinh. *J. Environ. Sci.* **25**, 348–356 (2013).
- Odum, J. R. *et al.* Aromatics, reformulated gasoline, and atmospheric organic aerosol formation. *Environ. Sci. Technol.* **31**, 1890–1897 (1997).
- European Commission (EC), *Directive 2008/50/EC of the European Parliament and of the Council of 21 May 2008 on Ambient Air Quality and Cleaner Air for Europe*, <http://eur-lex.europa.eu/LexUriServ/LexUriServ.do?uri=OJ:L:2008:152:0001:0044:EN:PDF> (2008).
- Chhabra, P. S., Flagan, R. C. & Seinfeld, J. H. Elemental analysis of chamber organic aerosol using an Aerodyne high-resolution aerosol mass spectrometer. *Atmos. Chem. Phys.* **10**, 4111–4131 (2010).
- Robinson, A. L. *et al.* Rethinking organic aerosols: semivolatile emissions and photochemical aging. *Science* **315**, 1259–1262 (2007).

16. Fuller, S. J., Wragg, F. P. H., Nutter, J. & Kalberer, M. Comparison of on-line and off-line methods to quantify reactive oxygen species (ROS) in atmospheric aerosols. *Atmos. Environ.* **92**, 97–103 (2014).
17. Donaldson, K. *et al.* Oxidative stress and calcium signaling in the adverse effects of environmental particles (PM₁₀). *Free Radic. Biol. Med.* **34**, 1369–1382 (2003).
18. McWhinney, R. D., Gao, S. S., Zhou, S. & Abbatt, J. P. Evaluation of the effects of ozone oxidation on redox-cycling activity of two-stroke engine exhaust particles. *Environ. Sci. Technol.* **45**, 2131–2136 (2005).
19. Mertes, P., Pfaffenberger, L., Dommen, J., Kalberer, M. & Baltensperger, U. Development of a sensitive long path absorption photometer to quantify peroxides in aerosol particles (Peroxide-LOPAP). *Atmos. Meas. Tech.* **5**, 2339–2348 (2012).
20. Surratt, J. D. *et al.* Chemical composition of secondary organic aerosol formed from the photooxidation of isoprene. *J. Phys. Chem. A* **110**, 9665–9690 (2006).
21. Spezzano, P., Picini, P. & Cataldi, D. Contribution of unburned lubricating oil and gasoline-derived n-alkanes to particulate emission from non-catalyst and catalyst-equipped two-stroke mopeds operated with synthetic lubricating oil. *J. Environ. Monit.* **10**, 1202–1210 (2008).
22. Santino, D., Picini, P. & Martino, L. Particulate matter emissions from two-stroke mopeds. *SAE* **2014**, 4–10 (2001).
23. Yang, C. J. Launching strategy for electric vehicles: Lessons from China and Taiwan. *Technol. Forecast. Soc. Change* **77**, 831–834 (2010).
24. Paulsen, D. *et al.* Secondary organic aerosol formation by irradiation of 1, 3, 5-trimethylbenzene-NO_x-H₂O in a new reaction chamber for atmospheric chemistry and physics. *Environ. Sci. Technol.* **39**, 2668–2678 (2005).
25. Chirico, R. *et al.* Impact of aftertreatment devices on primary emissions and secondary organic aerosol formation potential from in-use diesel vehicles: results from smog chamber experiments. *Atmos. Chem. Phys.* **10**, 11545–11563 (2010).
26. United Kingdom Transport Research Laboratory (TRL), *A Reference Book of Driving Cycles for Use in the Measurement of Road Vehicle Emissions*, http://www.trl.co.uk/online_store/reports_publications/trl_reports/cat_traffic_and_the_environment/report_a_reference_book_of_driving_cycles_for_use_in_the_measurement_of_road_vehicle_emissions.htm (2009).
27. Barnet, P. *et al.* OH clock determination by proton transfer reaction mass spectrometry at an environmental chamber. *Atmos. Meas. Tech.* **5**, 647–656 (2012).
28. Clairotte, M. *et al.* Online characterization of regulated and unregulated gaseous and particulate exhaust emission from two-stroke mopeds: a chemometric approach. *Anal. Chim. Acta.* **717**, 28–38 (2012).
29. Adam, T. *et al.* Chemical characterization of emissions from modern two-stroke mopeds complying with legislative regulation in Europe (EURO-2). *Environ. Sci. Technol.* **44**, 505–512 (2010).
30. Aiken, A. C. *et al.* O/C and OM/OC ratios of primary, secondary, and ambient organic aerosols with high-resolution time-of-flight aerosol mass spectrometry. *Environ. Sci. Technol.* **42**, 4478–4485 (2008).
31. Klaassen, G., Berglund, C. & Wagner, F. *The GAINS Model for Greenhouse Gases-Version 1.0: Carbon Dioxide (CO₂)*. IIASA Interim Report IR-05-53 (International Institute for Applied Systems Analysis (IIASA), Laxenburg, Austria, 2005).

Acknowledgements

This work was supported by the Swiss Federal Office for the Environment (FOEN), the Federal Roads Office (FEDRO), the Swiss National Science Foundation (Ambizione PZ00P2_131673, SAPMAV 200021_13016), the EU commission (FP7, COFUND: PSI-Fellow, grant agreement n.° 290605), the UK Natural Environment Research Council (NERC), the French Environment and Energy Management Agency (ADEME, Grant number 1162C0002) and the Velux Stiftung, project 593.

Author contributions

Study design (S.M.P., A.S.H.P., M.C., A.A.Z., U.B., I.E.H.); experimental work, idling 2S scooters (S.M.P., M.C., L.P., P.B., J.D., S.J.F.); experimental work, driving cycle 2S scooters and other vehicles (S.M.P., I.E.H., J.G.S., M.C., A.A.Z., S.H., B.T.-R. S.M.P., R.S.-B.); data analysis, emission factors (S.M.P., S.M.P., I.E.H., M.C., A.A.Z., J.G.S., P.B., S.H., B.T.-R.); data analysis, reactive oxygen species (S.J.F.); data analysis, SOA yields (S.M.P.); literature data ambient BTEX (R.-J.H.); literature data ambient PM/aromatic (I.E.H.); writing of manuscript (S.M.P.); preparation of display items (S.M.P., S.M.P., R.-J.H.); data interpretation and editing of manuscript (S.M.P., M.C., I.E.H., S.M.P., R.-J.H., R.Z., R.C., C.A., J.D., L.P., A.S.H.P., M.K., N.M., U.B.); comments and discussion on the manuscript (all).

Additional information

Supplementary Information accompanies this paper at <http://www.nature.com/naturecommunications>

Competing financial interests: The authors declare no competing financial interests.

Reprints and permission information is available online at <http://npg.nature.com/reprintsandpermissions/>

How to cite this article: Platt, S. M. *et al.* Two-stroke scooters are a dominant source of air pollution in many cities. *Nat. Commun.* 5:3749 doi: 10.1038/ncomms4749 (2014).